Self-Passivating Edge Reconstructions of Graphene

Pekka Koskinen,[1,*] Sami Malola,[1] and Hannu Häkkinen[1,2]

[1]*Department of Physics, NanoScience Center, 40014 University of Jyväskylä, Finland*
[2]*Department of Chemistry, NanoScience Center, 40014 University of Jyväskylä, Finland*

Planar reconstruction patterns at the zigzag and armchair edges of graphene were investigated with density-functional theory. It was unexpectedly found that the zigzag edge is metastable and a planar reconstruction spontaneously takes place at room temperature. The reconstruction changes electronic structure and self-passivates the edge with respect to adsorption of atomic hydrogen from a molecular atmosphere.

Carbon is one of the most prominent elements in nature, vital for biology and life. Although macroscopic carbon has been important since ancient times [1], only modern materials design, utilizing nanotubes [2,3], fullerenes [4], and single graphene sheets [5], fully attempts to use its flexible chemistry. In applications for nanoscale materials and devices, it is often the atomic and electronic structure of boundaries and surfaces that is responsible for mechanical, electronic, and chemical properties.

Since the properties of a nanomaterial depend on the precise atomic geometry, its knowledge is crucial for focused preparation of experiments and for worthy theoretical modeling. Only this enables the further development of nanoelectronic components, nanoelectromechanical devices, and hydrogen storage materials [3,6] or the usage of carbon in compound designs [7].

The importance of precise geometry is emphasized in low-dimensional systems. The strong correlations are known to bring up novel phenomena [8], and such should be expected also for the quasi-one-dimensional edges of graphene. The edge chemistry plays even a crucial role in the catalyzed growth of carbon nanotubes [9,10]. Specifically, as two-dimensional carbon has the honeycomb lattice, edge behavior ultimately boils down to the properties of graphene edges. Hence, it is relevant to explore different graphene edge geometries and their chemical properties beyond the standard zigzag and armchair ones.

This relevance is evident from the abundant literature. The electronic properties of graphene as well as carbon nanotube armchair and zigzag edges have been studied extensively [11,12], often in connection to nanotube growth [9,13] or the so-called electronic "edge states" [14–16]. There has been experimental and theoretical work done even on the reconstruction of graphene edges, but they have differed from the basic reconstruction patterns studied in this work. They have involved either edge roughness [15] or more dramatic folding of the edge into a loop [17].

The edges discussed in this work are shown in Fig. 1 and were investigated by modeling an infinitely long carbon nanoribbon of a given width (see methods). A tight-binding method [18] was used to explore a number of other edge candidates, but density-functional analysis only for the relevant ones is reported here. The most important edge is zz(57), a reconstruction of a zigzag edge where two hexagons transform into a pentagon and a heptagon, like
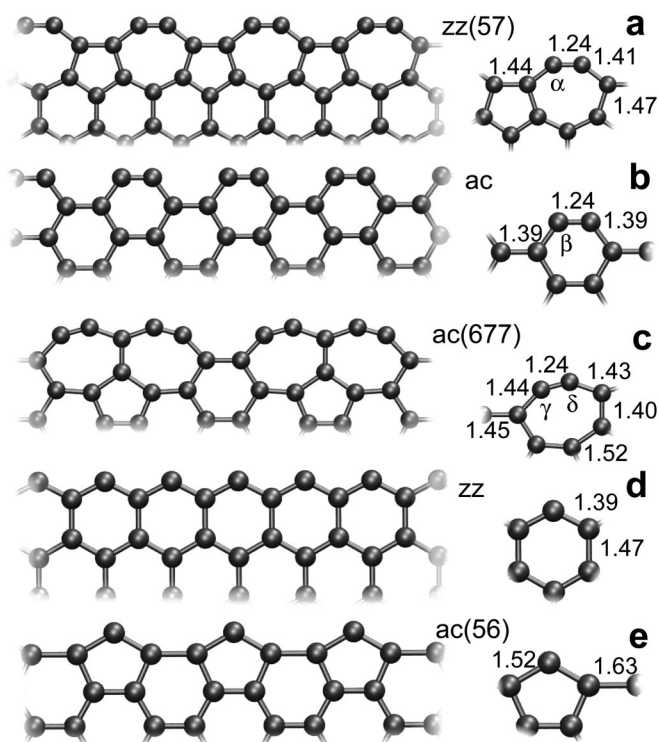

FIG. 1. The geometries of graphene edges: (a) reconstructed zigzag [zz(57)], (b) armchair (ac), (c) reconstructed armchair [ac(677)], (d) zigzag (zz), and (e) pentagonal armchair [ac(56)]. The numbers in parentheses denote the number of vertices in edge polygons. Some bond lengths (in Å) and bond angles are shown on the right: The bond angles are $\alpha = 143°$, $\beta = 126°$, $\gamma = 148°$, and $\delta = 147°$. All geometries are strictly in-plane.

an edge cut through a Haeckelite structure or a line of Stone-Wales defects [19]. The edge ac(677) is a reconstruction of the armchair edge where two separate ''armrest'' hexagons merge into adjacent heptagons by the Stone-Wales mechanism. The pentagonal reconstruction ac(56) of an armchair has a slightly different nature, since it requires the diffusion of carbon atoms from distant armrests to ''seat'' positions.

Let us start analysis by looking at edge energy ε_{edge}, which is calculated from the total energy of the graphene ribbon

$$E = -N\varepsilon_{gr} + L\varepsilon_{edge},$$

where N is the number of carbon atoms, L the total length of edges (twice the length of the simulation cell), and $\varepsilon_{gr} = 7.9$ eV is the cohesion energy of graphene. The edge energies converge rapidly as shown in Fig. 2 and justify the reference to (semi-infinite) graphene. The energy of the armchair edge is 0.33 eV/Å lower than for the zigzag edge, in accord with a similar value for nanotubes [10]. However, the principal result is that by edge reconstruction the zigzag may lower its energy by 0.35 eV/Å. This implies that the reconstructed zigzag is the best edge for graphene. To the best of our knowledge, this is the first report on the metastability of the zigzag edge, which is surprising in view of the abundant literature. Thermal stability of this novel reconstruction was also confirmed with tight-binding simulations [18]. The ac(677) edge has only slightly higher energy than the armchair edge, whereas ac(56) reconstruction has the highest edge energy. We remark that the reconstructions appear to be stable with respect to out-of-plane motion, a situation somewhat different from small-diameter nanotubes [9,13].
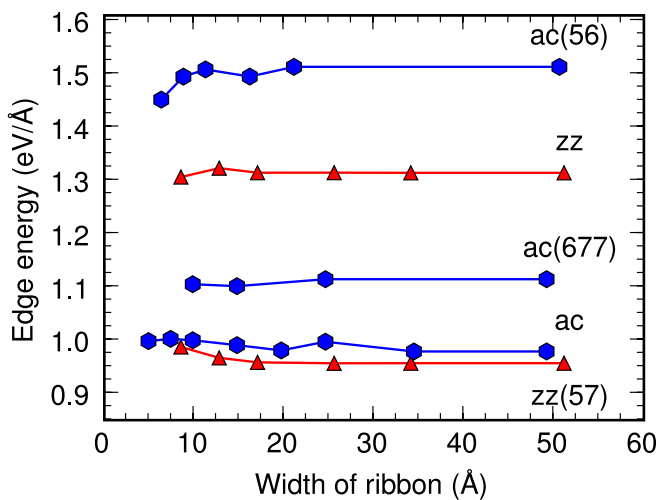
These energetics can be understood by looking at the geometries of Fig. 1. Previous studies have shown that the armchair has low energy due to triple bonds in the armrests [12], as realized by comparing their short bonds (1.24 Å) to the bond in acetylene (1.20 Å). The zigzag does not have such triple bonds and ends up with strong and expensive dangling bonds. The reconstructed zz(57) has triple bonds (1.24 Å) but also wider bond angles (143°) which reduces the hybridization energy cost. Triple bonds with wide angles can be observed also in the ac(677) edge, but strain in other parts makes the reconstruction unfavored. The ac(56) edge suffers from dangling bonds like zigzag, and additional high strain energy makes this reconstruction the most expensive one. Regardless, the ac(56) edge has relevance during the growth of armchair edges [10].

These observations are supported by hydrogen atom adsorption energies, shown in Fig. 3. The weak adsorption for the armchair (4.36 eV) compared to the zigzag (5.36 eV) stems from the triple bonds in the armchair edge. Similarly, the weak adsorption for zz(57) (3.82 eV) and ac(677) (3.64 eV) witnesses the weakening of dangling bonds. The adsorption for ac(56) is large because of the strongest dangling bonds. For insight, the adsorption energies in Fig. 3 are replotted by subtracting hydrogen molecule binding energy $E_{H_2} = 4.58$ eV. The resulting negative number for zz(57) means that the adsorption of hydrogen atom from the H_2 molecule is not favored due to the cost of H_2 dissociation energy, unless the adsorption process should be complicated [20]. This amounts to the conclusion that the edge reconstruction chemically passivates the zigzag edge. However, hydrogen adsorption for
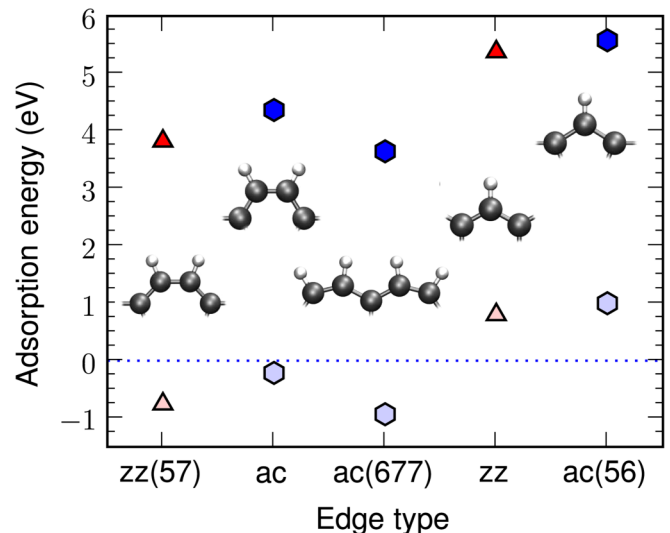

FIG. 2 (color online). The edge energies of carbon nanoribbons. Energies are plotted as a function of the ribbon width for the edges in Fig. 1.

FIG. 3 (color online). Hydrogen adsorption energies. The upper symbols correspond to ε_{ads} with coverage of one hydrogen per edge atom, and lower faint symbols are shifted by subtracting the H_2 binding energy; positive $\varepsilon_{ads} - E_{H_2}$ means the hydrogen atom is more strongly bound to the edge than to the H_2 molecule.

TABLE I. Summary of the edge and hydrogen adsorption energies. ε_{edge}^* is the energy per edge atom, ε_{ads} is the hydrogen adsorption energy with full edge coverage, and $\varepsilon_{edge+ads}$ is the edge energy with hydrogen termination. Note that for ac(56) the edge atom density is $\lambda_{ac(56)} = \lambda_{ac}/2$.

Edge	zz(57)	ac	ac(677)	zz	ac(56)
ε_{edge} (eV/Å)	0.96	0.98	1.11	1.31	1.51
ε_{edge}^* (eV/atom)	2.36	2.09	2.30	3.22	6.43
ε_{ads} (eV)	3.82	4.36	3.64	5.36	5.58
$\varepsilon_{edge+ads}$ (eV/Å)	0.34	0.01	0.45	0.06	0.74

the zigzag + hydrogen edge has a yet smaller adsorption energy of 2.14 eV.

The edge energetics are summarized in Table I. Note that the ordering of edges changes when expressed as energy per edge atom ($\varepsilon_{edge}^* = \varepsilon_{edge}\lambda^{-1}$) due to different edge atom densities $\lambda_{ac} = (2.13 \text{ Å})^{-1}$ and $\lambda_{zz} = (2.46 \text{ Å})^{-1}$. More interesting is to look at edges with hydrogen termination (Klein edge) [16]. For this case the edge energy is $\varepsilon_{edge+ads} = \varepsilon_{edge} - \lambda(\varepsilon_{ads} - E_{H_2}/2)$, where the reference is to bulk graphene and H_2 molecules. The best edges in this case are normal armchair and zigzag edges because of dangling bonds. On the contrary, the weak dangling bonds and small adsorption energy cause high energies for zz(57) and ac(677) Klein edges.

Let us now concentrate on the thermodynamic and electronic properties of zigzag edges. We would like to clarify an aspect which is ambiguous in the literature: There are two types of electronic zigzag edge states. The so-called "flat band" in Fig. 4(a) comes from the bulk π electrons and is indeed localized at the edge. But the band due to dangling bonds is the one seen in the scanning tunneling microscope (STM) image and is located spatially even beyond the edge [Fig. 4(c)]. In zz(57), formation of triple bonds is evidenced by the nearly isolated dimers in Fig. 4(d), and the reconstruction removes the dangling bond bands away from the Fermi level by lifting the degeneracy almost by 5 eV. Hence, for zz(57) the STM image shows only the flat band states. Because the dangling bond bands shift to elusive energies, chemical reactivity also reduces.

In a thermodynamic sense, the spontaneous reconstruction of the zigzag into zz(57) should be possible, since the activation barrier from the zigzag side is only 0.6 eV, from the reconstructed side 2.4 eV. The G-mode vibration of graphene at 1580 cm^{-1} gives an attempt frequency of $\nu_G \sim 5 \times 10^{12}$ s^{-1}, and an elementary approach yields the rapid rate $\nu_G \exp(-E_B/k_BT) \approx 4 \times 10^2$ s^{-1} at room temperature.

The reconstructions predicted in this work are expected to survive on graphite terraces due to the weak interaction (5.6 meV/atom) between the basal planes [21]. By using appropriate sample preparation, it should be thus possible to observe the reconstruction. STM images often show
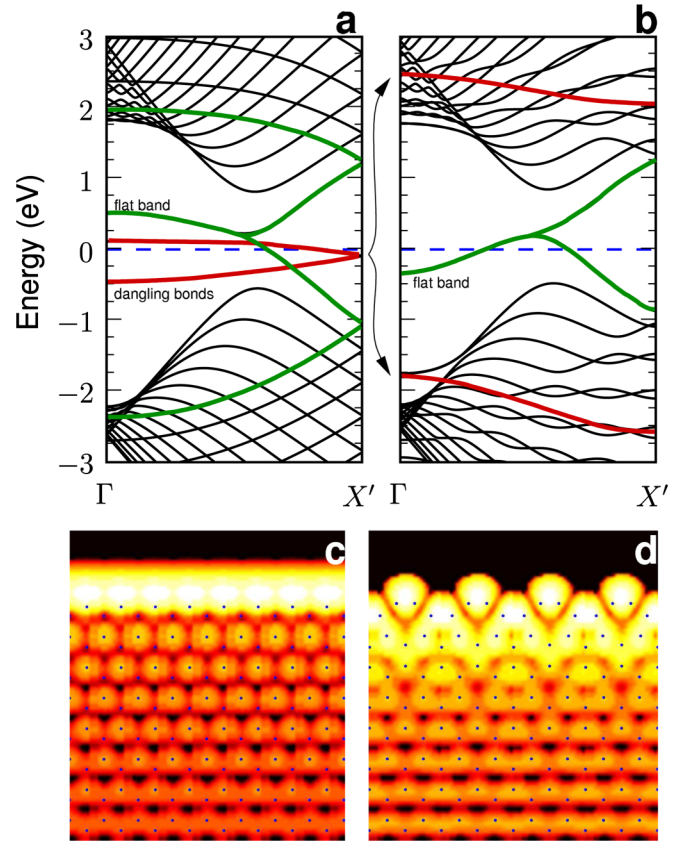

FIG. 4 (color online). The electronic structure of zigzag and zz (57) edges. (a) and (b) show the band structure for 34 Å wide zigzag and zz(57) nanoribbons, respectively, with a unit cell width of 4.9 Å. Note that for the zigzag this is twice the minimum unit cell, and the reciprocal space is thus only half of the normal representation. The dashed line is the Fermi level. The colored (thick) bands were identified directly by visual inspection of the wave functions. (c) and (d) show the height profiles of simulated scanning tunneling microscope images in the constant current mode of the respective edges (height variations >2 Å), formed by integrating the electron density from occupied bands within 0.1 eV of the Fermi energy. The degeneracies at the gamma point are 2 and 4 for the dangling bonds and the flat band, respectively.

irregular and blurred edges, yielding no atomic resolution, but at least for passivated edges armchair predominance is claimed, in agreement with Table I [16,22]. So far, samples have been prepared intentionally with hydrogen passivation during heat treatment [22,23], a situation where reconstruction would not be favored. Alternate routes for observing the reconstruction would be the radial distribution function from neutron diffraction experiments without a deuterium atmosphere [23] or detection of triple bond-spawned high-energy modes around 2000 cm^{-1} with Raman spectroscopy.

A further topic is the study of the conductance of various graphene edges, particularly the zz(57) edge found here. The presence of the edge state around the Fermi level makes zz(57) ideal for conductance measurements, in con-

trast to armchair ribbons where the edge state is absent. This may render zz(57) as an interesting stable model for quasi-one-dimensional carbyne with alternating single and triple bonds. Furthermore, the novel thermodynamically and chemically stable reconstruction could play a role in the formation of angular joints in nanoribbons [24], closure of the ends of nanotubes after cutting [25], and any other system where graphene sheets are joined to produce systems with nanoscale morphology.

Methods.—We used density-functional theory in conjunction with the generalized gradient approximation for the exchange correlation functional [26] and projector augmented waves [27] for the C($2s2p$) electrons, as implemented in GPAW code using real-space grids [28]. Converged energies were obtained with grid spacing of 0.2 Å and 10 **k** points in the periodic direction. In the perpendicular directions, the system is not periodic, and the space between the atoms and the wall of the simulation cell was $\geq$ 5.0 Å. The energies were converged to $\sim 10^{-5}$ eV/atom, and structures were optimized until forces were less than 0.05 eV/Å. Our calculations agree well with previous relevant experimental as well as theoretical energetic and geometric properties [12,21]. The activation barrier was calculated with the nudged elastic band method [29,30] by fixing the atoms beyond the first two zigzag rows with a unit cell of length 4.9 Å. The constant current STM of Fig. 4 shows the height profile of the electron density isosurface of the occupied states within an $\sim$0.1 eV energy window below the Fermi level. The isosurface value corresponds to an average density 2 Å above the graphene plane (3×10^{-5} electrons/ Å^3).

*To whom correspondence should be addressed.
pekka.koskinen@phys.jyu.fi

[1] M. I. Katsnelson, Mater. Today **10**, 20 (2007).
[2] S. Ijima, Nature (London) **354**, 56 (1991).
[3] R. H. Baughman, A. A. Zakhidov, and W. A. de Heer, Science **297**, 787 (2002).
[4] H. W. Kroto, J. R. Heath, S. C. O'Brien, R. F. Curl, and R. E. Smalley, Nature (London) **318**, 162 (1985).
[5] J. C. Meyer, A. K. Geim, M. I. Katsnelson, K. S. Novoselov, T. J. Booth, and S. Roth, Nature (London) **446**, 60 (2007).
[6] J. M. Kinaret, T. Nord, and S. Viefers, Appl. Phys. Lett. **82**, 1287 (2003).
[7] S. Stankovich, D. A. Dikin, G. H. B. Dommet, K. M. Kohlhaas, E. J. Zimney, E. A. Stach, R. D. Piner, S. T. Nguyen, and R. S. Ruoff, Nature (London) **442**, 282 (2006).
[8] P. Koskinen, H. Häkkinen, B. Huber, B. von Issendorff, and M. Moseler, Phys. Rev. Lett. **98**, 015701 (2007).
[9] J.-C. Charlier, A. De Vita, X. Blase, and R. Car, Science **275**, 647 (1997).
[10] Y. H. Lee, S. G. Kim, and D. Tomanek, Phys. Rev. Lett. **78**, 2393 (1997).
[11] K. Nakada, M. Fujita, G. Dresselhaus, and M. S. Dresselhaus, Phys. Rev. B **54**, 17 954 (1996).
[12] T. Kawai, Y. Miyamoto, O. Sugino, and Y. Koga, Phys. Rev. B **62**, R16 349 (2000).
[13] E. Hernandez, P. Ordejon, I. Boustani, A. Rubio, and J. A. Alonso, J. Chem. Phys. **113**, 3814 (2000).
[14] D. Jiang, B. G. Sumpter, and S. Dai, J. Chem. Phys. **126**, 134701 (2007).
[15] D. Gunlycke, D. A. Areshkin, and C. T. White, Appl. Phys. Lett. **90**, 142104 (2007).
[16] Y. Kobayashi, K.-I. Fukui, T. Enoki, and K. Kusakabe, Phys. Rev. B **73**, 125415 (2006).
[17] K. Jian, A. Yan, I. Kulaots, G. P. Crawford, and R. Hurt, Carbon **44**, 2102 (2006).
[18] D. Porezag, T. Frauenheim, T. Köhler, G. Seifert, and R. Kaschner, Phys. Rev. B **51**, 12 947 (1995).
[19] A. J. Stone and D. J. Wales, Chem. Phys. Lett. **128**, 501 (1986).
[20] X. Sha and B. Jackson, J. Am. Chem. Soc. **126**, 13 095 (2004).
[21] X. Hua, T. Cagin, J. Che, and W. A. Goddard III, Nanotechnology **11**, 85 (2000).
[22] Y. Kobayashi, K.-I. Fukui, T. Enoki, K. Kusakabe, and Y. Kaburagi, Phys. Rev. B **71**, 193406 (2005).
[23] T. Fukunaga, K. Itoh, S. Orimo, M. Aoki, and H. Fujii, J. Alloys Compd. **327**, 224 (2001).
[24] X. Li, X. Wang, L. Zhang, S. Lee, and H. Dai, Science **319**, 1229 (2008).
[25] Y. Gan, J. Kotakoski, A. V. Krasheninnikov, K. Nordlund, and F. Banhart, New J. Phys. **10**, 023022 (2008).
[26] J. P. Perdew, K. Burke, and M. Ernzerhof, Phys. Rev. Lett. **77**, 3865 (1996).
[27] P. E. Blöchl, Phys. Rev. B **50**, 17 953 (1994).
[28] GPAW wiki, https://wiki.fysik.dtu.dk/gpaw.
[29] G. Henkelman and H. Jonsson, J. Chem. Phys. **113**, 9978 (2000).
[30] E. Bitzek, P. Koskinen, F. Gähler, M. Moseler, and P. Gumbsh, Phys. Rev. Lett. **97**, 170201 (2006).